Tellus (1988), *40A*, 120–132

Intraseasonal fluctuations in low-level meridional winds over the Indian Ocean and monsoonal convection over South Asia*

By MADAN L. SHRESTHA[1] and TAKIO MURAKAMI, *Department of Meteorology, University of Hawaii, 2525 Correa Road, Honolulu, Hawaii 96822, USA*

(Manuscript received 26 January; in final form 30 April 1987)

ABSTRACT

Some aspects of 30–60 day meridional wind fluctuations over the mid-latitude Indian Ocean were investigated using lag correlation maps for the 5 summers of 1979–1983. At times, the equatorial low-frequency (30–60 day) modes exhibit a systematic eastward propagation. However, they are occasionally interrupted by irregular movements or even westward propagation. This study concentrates only on those periods with a systematic eastward propagation and a well-defined tropical–extratropical atmospheric teleconnection pattern.

Low-level meridional wind fluctuations in the low-frequency domain are prominent over the western Indian Ocean off the east coast of Africa. The anomalous southerly flows, which are initiated around northern Madagascar move northward and, after crossing the equator, contribute to the intensification of the monsoonal westerlies over South Asia, thus, enhancing convection over the monsoon region. In comparison, 30–60 day southerlies (anomaly) over the eastern Indian Ocean off the west coast of Australia tend to enhance equatorial convection over the western Pacific between about 150°E and the date line.

Perturbations with periods shorter than 30 days are considered transient disturbances. Spectral analysis of transient eddy kinetic energy in the extratropical regions reveals a significant peak in the low-frequency range. This is associated with an amplitude modulation of transient disturbances. Thus, it is plausible that transient disturbances, as a group, provide energy for the enhancement of 30–60 day planetary-scale perturbations over the subtropics.

1. Introduction

Since the detection of low-frequency modes by Madden and Julian (1971, 1972), substantial work has been done on the investigation into their temporal and spatial behavior. These perturbations have a zonal wave number one feature and an eastward speed of 8° longitude per day (Lorenc, 1984; Krishnamurti et al., 1985). Furthermore, these eastward propagating modes tend to intensify substantially after reaching the Asian monsoon region. Using outgoing longwave radiation (OLR) data, Murakami et al. (1986a) found the predominance of 30–60 day oscillation over the equatorial Indian Ocean east of 60°E and the Pacific Ocean west of the date line. Thus, the 30–60 day oscillations are unique to the equatorial eastern hemisphere. Such a large regional difference in the low-frequency perturbations reflects the important rôle played by the localities over which they lie. Perhaps, the observed 30–60 day oscillations can be regarded as forced waves. On the other hand, the numerical experiment conducted by Hayashi and Sumi (1986) assuming an ocean-covered earth in the general circulation model found a prominent eastward propagating wave with a periodicity of 30 day and a zonal wavenumber one within about 10° latitude of the equator. In the experiment no

* Contribution no. 87-03, Department of Meteorology, University of Hawaii, USA.

[1] Present affiliation: Nepal Meteorological Service, Kathmandu, Nepal.

external forcing was prescribed and the wave modes were internally enhanced by convection. Thus, these simulated waves can be identified as "free mode (normal mode)" of the equatorial region.

The atmospheric teleconnections between the Indian monsoon system and the northern hemisphere westerly regime was investigated by Yasunari (1986). On the other hand, several investigators (e.g., Yasunari, 1980; Knutson et al., 1986) detected the occurrence of systematic northward propagation of 30–60 day perturbations which originate in the equatorial Indian Ocean and dissipate near the foothills of the Tibetan Plateau. Yasunari (1981) further conjectured that the enhancement of low-frequency modes over South Asia is linked, in some way, to periodical cold air outbreaks from the southern hemisphere extratropics. Recently, Murakami (1987) showed that 30–60 day southerlies (anomaly) from the southern hemisphere middle latitudes at the 850 mb level tend to cause widespread convection throughout the entire Asiatic monsoon domain during the northern hemisphere summer. These southerlies correspond to the low-level branch of an anomalous (30–60 day) Hadley circulation. In this paper, an attempt is made to further examine the relationship between these southerlies from the southern hemisphere middle latitudes and the enhancement of convection over the Asiatic monsoon region. In addition, the interaction of transient disturbances (period less than 30 days) with low-frequency oscillations is also investigated.

2. Data and computational procedures

In this study, daily wind (u, v) and geopotential height (Φ) data at 850 mb are utilized over the global region between 65°S–65°N with 2.5° latitude/longitude resolution during the 5 northern hemisphere summers (1 May–30 September) of 1979 to 1983. These data were extracted from operational analyses at the European Centre of Medium Range Weather Forecasts (ECMWF). Daily outgoing longwave radiation (OLR) data obtained from polar orbiting satellites between 45°S and 45°N were also used. These OLR data were derived by averaging the daytime and nighttime observations.

Applying harmonic analysis to the data, the yearly and half-yearly components were computed. The sum of these two components mainly accounts for the seasonal cycle. The seasonal cycle and the annual mean are grouped together and designated by the notation $\langle\ \rangle$. Thus, the departure of u from $\langle u \rangle$ is given by

$$u' = u - \langle u \rangle. \tag{1}$$

A band-pass filter is then applied to u' according to the procedure outlined by M. Murakami (1979) to extract 30–60 day filtered data. These filtered data are denoted by $(\tilde{\ })$. Thus, we can write u' as

$$u' = \tilde{u} + u^*, \tag{2}$$

where u^* is the transient component with periods less than 30 days.

Though the general tendency of the 30–60 day perturbations is to propagate eastward, they are often interrupted by irregular movements or sometimes even westward propagation. Fig. 1 depicts a time–longitude section of $\widetilde{\text{OLR}}$ averaged within the latitude belt 0°–10°N from 50°E to 180°. There are some periods when the eastward propagation is clearly defined; for example, 1 May–2 September 1979; 16 June–20 July and 29 August–20 September 1980; 10 July–30 September 1981; 9 June–30 September 1982; 4 June–7 July 1983. These periods of eastward propagation are designated as "E". In Fig. 1, heavy arrows indicate E phases. The periods of irregular movement are signified as "NE". The total number of days for E (NE) phase is 414 (351) days for the 5 summers. The reader is directed to Murakami's (1987) paper for the large difference in the nature of low-frequency oscillations between the two contrasting phases. The summertime tropical–extratropical teleconnection is more clearly defined in E phase than in NE phase. This paper concentrates on the further investigation into the atmospheric teleconnections associated with low-frequency perturbations during E phase.

An out-of-phase relationship between $\widetilde{\text{OLR}}$ over the equatorial Indian Ocean (80°E) and the western Pacific (140°E) is evident in Fig. 1. During the E phase of the 1981 summer, when the equatorial Indian Ocean experiences wet conditions (denoted by W), the western Pacific is dominated by dry weather (denoted by D).

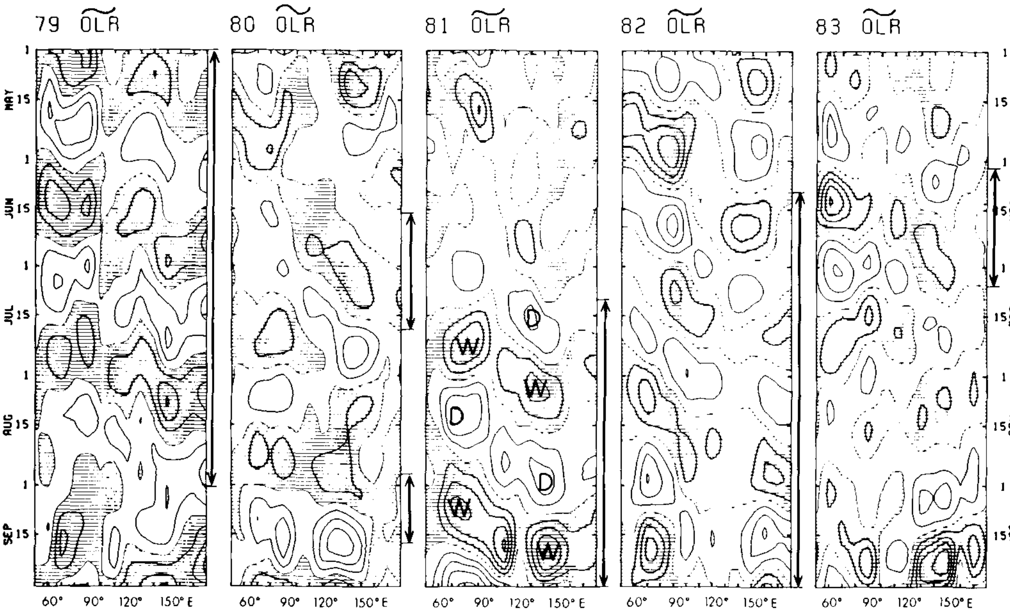

Fig. 1. Time-longitude sections of 30–60 day filtered $\widetilde{\text{OLR}}$ averaged between the equator and 10°N from 50°E to the date line during the 5 summers (1 May–30 September) of 1979 to 1983. Intervals are 10 W m^{-2} with negative anomaly shaded. W (D) denotes peak wet (dry) period. Heavy arrows indicate E phases with systematic eastward propagation.

Conversely, when the equatorial Indian Ocean is dry, the western Pacific is wet. This dipole feature in the convective activity has been observed by previous investigators (Lau and Chan, 1985; Murakami et al., 1986a).

The primary objective of this study is to investigate the rôle of mid-latitude effects upon the enhancement of convection over the equatorial monsoon region utilizing one-point correlation maps with reference to 30–60 day $\tilde{\Phi}$ fluctuations over several key areas. To test the significance of one-point correlation coefficients, the effective number of degree of freedom is computed according to Davis (1976). Based on this degree of freedom, the local correlation coefficients greater (less) than 0.3 (-0.3) are significant at 95% confidence level. For brevity, the areal percentage that surpasses the local 95% confidence level is signified as "LS". In order for a correlation map to be globally significant, LS should exceed certain critical value. The global significance is determined by the same procedure as described by Lau and Phillips (1986). The reader is directed to their paper for a complete development of the statistical test, as only a brief outline will be presented here. The 30–60 day filtered $\tilde{\Phi}$ data at the reference point were replaced by randomly selected numbers from the 30–60 day filtered maps. Thus, these randomly selected numbers preserve some information on spatial degrees. A Monte Carlo experiment consisting of 400 independent trials was performed, each with different random numbers at the reference point. The correlation between the random time series and the 30–60 day filtered data at every grid point was computed. The percentage area occupied by locally significant correlations for a 95% global significance was determined from the histogram of the Monte-Carlo experiment. This globally significant percentage area is hereafter denoted as "GS". A correlation map is considered to be globally significant if LS for this particular correlation map is greater than GS. As mentioned earlier, all correlation maps to be presented in this paper are for E phase. It turns out that the majority of the correlation maps for E phase surpass the 95% global confidence level (LS > GS). The high statistical significance of correlation maps can be explained as follows: the correlations were computed only for the E phase. In comparison, the correlations for the entire 5 years (1979–1983) of data would combine entirely different flow regimes together; thereby, masking the distinct characteristics of both the E and NE phase.

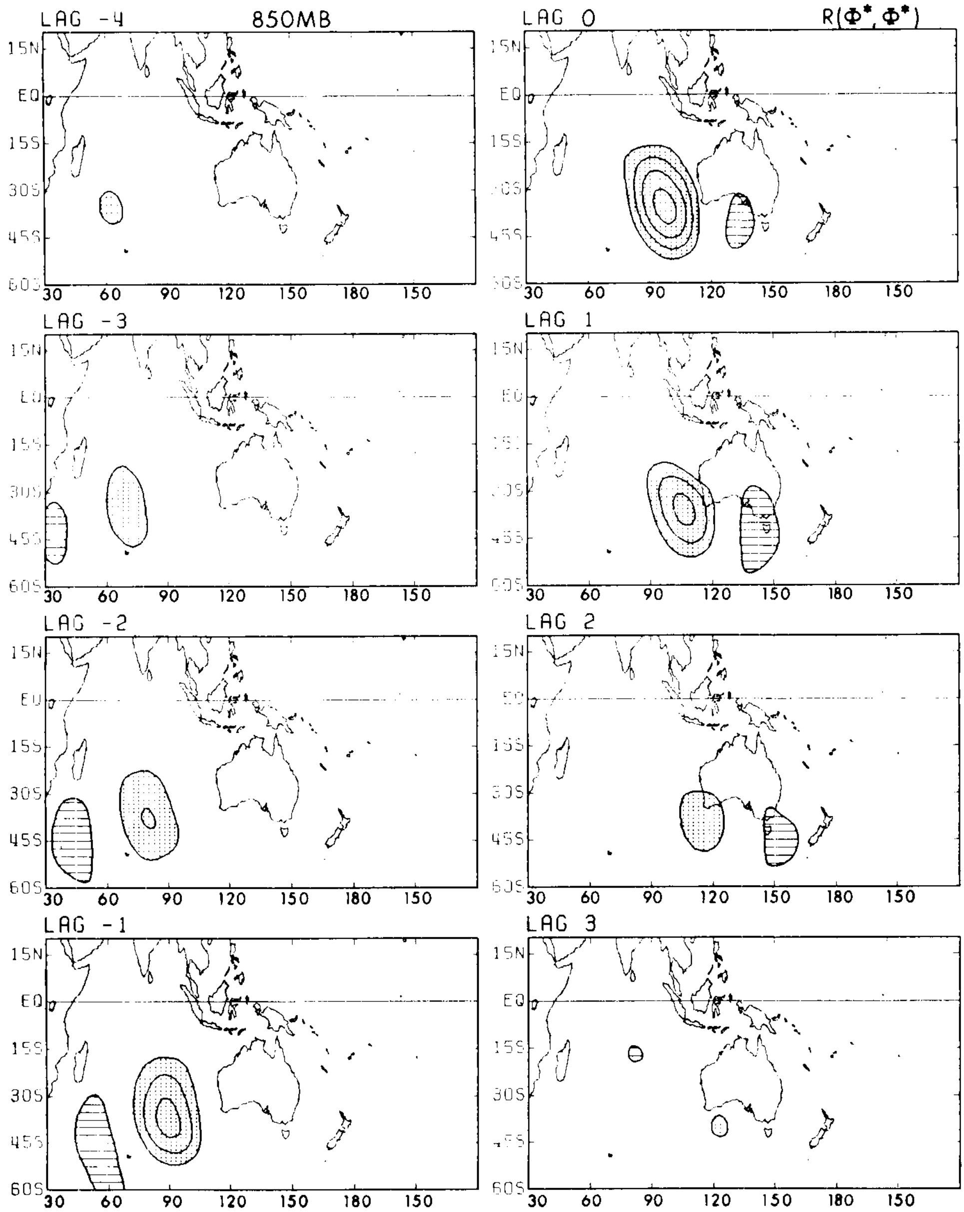

Fig. 2. Lag correlation of transient geopotential height Φ* at 850 mb with reference to the area average Φ* over the eastern Indian Ocean (90°–110°E, 30°–40°S) for lags −4, −3, . . ., and 3. Intervals are 0.2 and areas of correlation coefficient greater (less) than 0.3 (−0.3) are stippled (hatched).

3. Correlation patterns for transient disturbances

Fig. 2 shows the lag correlation of transient geopotential height (Φ^*) at 850 mb. Here, the areal average of Φ^* over the eastern Indian Ocean (90°–110°E, 30°–40°S) was taken as a reference. As shown by Murakami (1987), this region represents a key area for the occurrence of cold southerly surges bursting out of the southern hemisphere mid-latitude region. In this paper, the terms "correlation" and "anomaly" are used interchangeably. Regions with a local correlation coefficient significant at the 95% confidence level are shaded. Although the lag correlation was computed over the entire globe, it surpasses the confidence level only in the immediate vicinity of the reference point. Thus, the correlation pattern exhibits regional aspects of transient disturbances propagating eastward across the Indian Ocean. At lag -4 days, a small area of positive correlation is observed around 60°E, 35°S, which shifts eastward reaching 70°E by lag -3. At the same time an opposite anomaly area is observed near 35°E. This pair of positive and negative anomalies propagates systematically eastward. At lag 0 day, when the positive correlation is maximum (1.0) at the reference point, an opposite anomaly area is observed south of Australia around 135°E, 40°S. These anomalies have an approximate wave length of 6000 km and an average phase speed of about 10 m s^{-1}. This feature reflects the nature of middle latitude baroclinic disturbances superimposed upon the jet stream during the southern hemisphere winter.

Correlation patterns computed with reference to Φ^* at different locations (for example, the Bay of Bengal and the western North and South Pacific) also show regional aspects of transient disturbances. Thus, no extensive atmospheric teleconnection occurs in the transient time-scale of less than 30 days.

4. Correlation patterns for 30–60 day perturbations

The nature of 30–60 day filtered geopotential height ($\tilde{\Phi}$) perturbations are investigated utilizing lag-correlation patterns with reference to 850 mb $\tilde{\Phi}$ variations over central India (70°–90°E, 15°–25°N). This is presented in Fig. 3 for lags -10, -5, 0, and 5 days. Unlike the correlation maps for transient disturbances, the 30–60 day $\tilde{\Phi}$ correlation patterns show a distinct global-scale character. Using the criteria described in Section 2, these lag correlation patterns are all globally significant at the 95% confidence level and provide much useful information pertaining to the global-scale 30–60 day atmospheric teleconnection during the northern hemisphere summer. Lag correlations were also computed for different variables with reference to several key areas, including $\tilde{\Phi}$ over eastern Australia (30°S, 150°E). The horizontal configuration of computed lag correlations is essentially identical to the correlation patterns shown in Fig. 3 and, thus, is not reproduced here.

The lag 0 correlation (Fig. 3c) is positive over a large area extending southeastward from the eastern Mediterranean Sea across central India, the maritime continent and Australia, to New Zealand. At the same time a large negative region stretches from the Aleutian Islands through Mexico to the southwestern Atlantic off the east coast of Brazil. These anomalous patterns are characterized by a zonal wave number 1 with a distinct NW-SE tilt from 50°N to 50°S, indicating a close link between the northern and southern hemisphere extratropics. Here, it should be noted that Fig. 3c indicates two anomalous patterns since the $\tilde{\Phi}$ perturbations over central India may be either positive or negative. As Murakami and Nakazawa (1985) showed, the occurrence of negative (positive) $\tilde{\Phi}$ anomalies at 850 mb over central India corresponds to the time of active (break) monsoon. For brevity, a description of correlation patterns is given for the case when the monsoon is active over the central Indian region. Here, 30–60 day $\tilde{\Phi}$ perturbations become anomalously low not only over India, but also over the maritime continent and the Australian subcontinent (refer to the lag 0 correlation map). This anomalous $\tilde{\Phi}$ configuration indicates southerly flows (anomaly) along the western coast of Australia extending northwestward to the western equatorial Indian Ocean. These 30–60 day southerlies are schematically delineated by heavy dots in Fig. 3c for lag 0. Similarly, 30–60 day southerlies occurring during lags -10 and -5 are indicated in Figs. 3a and b, respectively. It appears that the 30–60 day south-

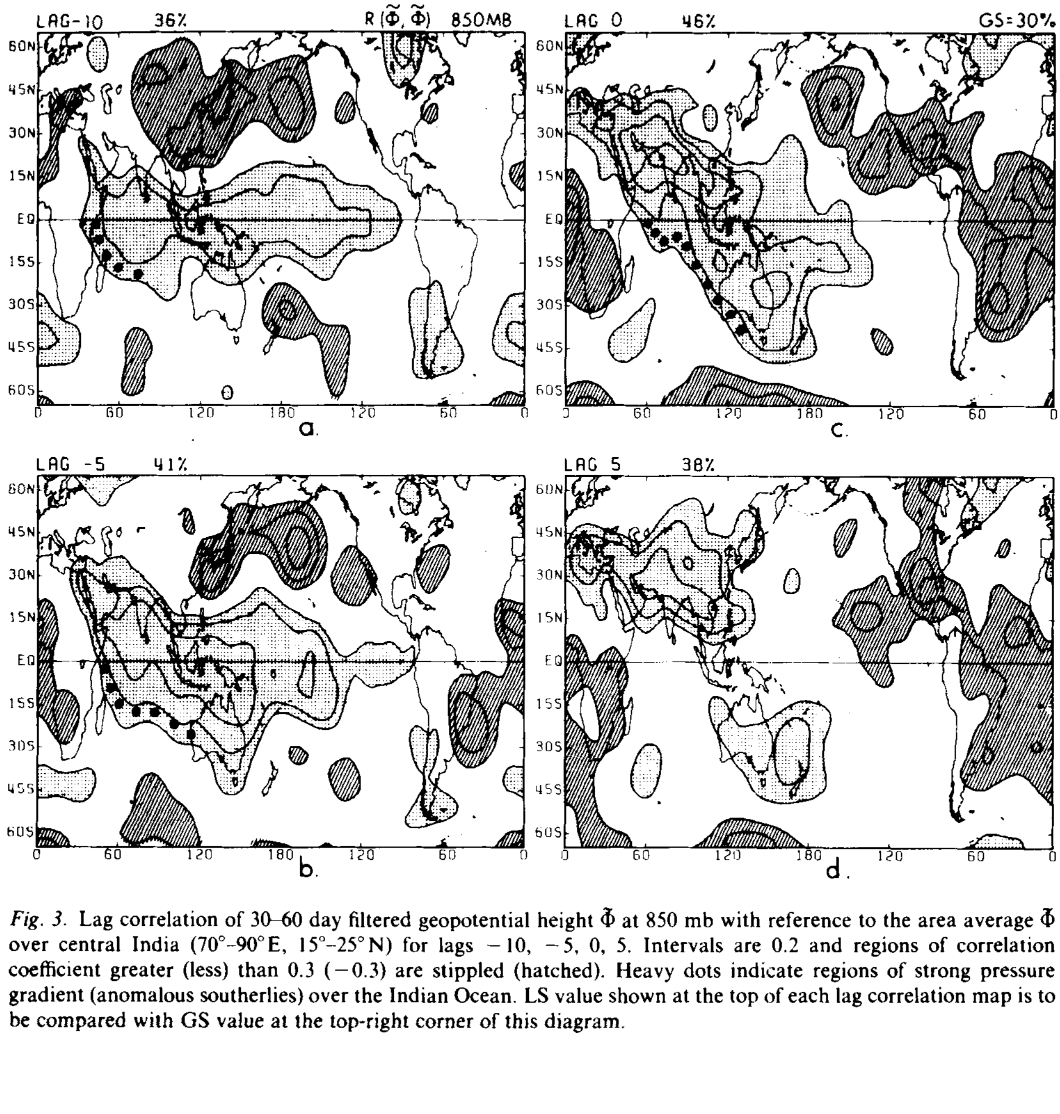

Fig. 3. Lag correlation of 30–60 day filtered geopotential height $\tilde{\Phi}$ at 850 mb with reference to the area average $\tilde{\Phi}$ over central India (70°–90° E, 15°–25° N) for lags −10, −5, 0, 5. Intervals are 0.2 and regions of correlation coefficient greater (less) than 0.3 (−0.3) are stippled (hatched). Heavy dots indicate regions of strong pressure gradient (anomalous southerlies) over the Indian Ocean. LS value shown at the top of each lag correlation map is to be compared with GS value at the top-right corner of this diagram.

erly flows from the southern hemisphere middle latitudes play an important rôle in the enhancement of convection over the Asiatic monsoon region. This aspect will be further elaborated on later.

The −10 day lag correlation map exhibits near symmetric character with respect to the equator. This is most clearly defined over the Indian Ocean-Pacific region from about 40° E to 100° W, where an E-W extended zone of positive correlation along the equator is sandwiched between a pair of negative correlation zones stretching along 45° N and 45° S, respectively. Of interest is the presence of large negative correlation (< −0.5) over southern China and Japan. Namely, the Baiu activity over these regions tends to be depressed below normal about 10 days prior to the initiation of active monsoons over central India.

After lag −10, regions of positive correlation over the equatorial Indian Ocean shifts northward across the Arabian Sea and the Bay of Bengal.

Recently, several investigators documented the northward propagation of low-frequency modes in association with the phase changes between active and break monsoons over India (Yasunari, 1980; Sikka and Gadgil, 1980; Krishnamurti and Subrahmanyam, 1982; M. Murakami, 1984; T. Murakami et al., 1984). As regions of positive correlation reach central India by lag 0 day, negative anomalies are found over the eastern Pacific–Central America–eastern Brazil region, in agreement with the findings by Murakami and Nakazawa (1985).

To further investigate the rôle of 30–60 day southerlies (anomaly) from the mid-latitude Indian Ocean, the lag correlation $R(\tilde{\Phi}, \tilde{v})$ for $\tilde{v}$ fields was computed with reference to filtered 850 mb geopotential height ($\tilde{\Phi}$) over central India. The correlation map for lag 0 (Fig. 4c) is globally significant at the 95% confidence level. For lags −10, −5, and +5 days, however, LS is less than GS and, thus, these lag correlation patterns are not globally significant at the 95% confidence level. Yet, they exhibit some interesting regional aspects of 850 mb $\tilde{v}$ perturbations that surpass the local 95% confidence level. At lag −10 days (Fig. 4a), a negative region is observed in the western Indian Ocean to the north of Madagascar. This area shifts systematically northward reaching the

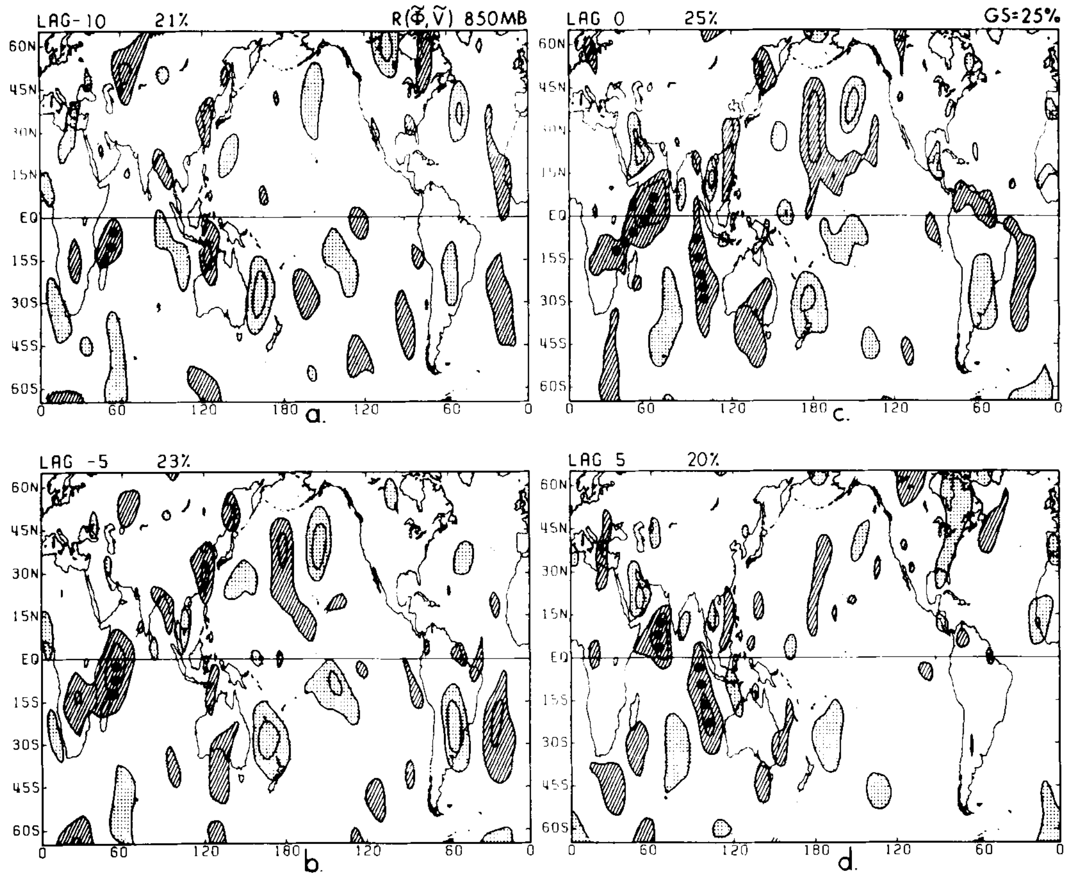

Fig. 4. As in Fig. 3, except for the lag correlation of meridional wind $\tilde{v}$ with reference to the area average geopotential height $\tilde{\Phi}$ over central India.

Arabian Sea in the northern hemisphere by lag −5. When the reference area (central India) is occupied by low $\tilde{\Phi}$ pressure at day 0, the east coast of Africa is dominated by southerly cross-equatorial flows. These southerly $\tilde{v}$ flows undoubtedly contribute to activate convection over the monsoon area. Significant southerlies are also apparent over the eastern Indian Ocean west of Australia. In the correlation map for lag 0 (Fig. 4c), two main branches of southerly $\tilde{v}$ flows are indicated by heavy dots. Southerly flows over the eastern Indian Ocean become dominant after lag 0, reaching maximum at 5 day lag. These anomalous southerlies tend to enhance equatorial convection over the western Pacific between about 150°E and the date line. To demonstrate this, the lag correlation coefficients of equatorial O$\tilde{L}$R averaged between 0° and 10°N from 30°E to 120°W are computed with reference to $\tilde{v}$ over two regions: one over the eastern Indian Ocean (30°–40°S, 100°–110°E) and the other over the western Indian Ocean (10°–20°S, 40°–60°E). Fig. 5a shows a systematic eastward propagation of equatorial O$\tilde{L}$R perturbations. It is interesting to note that about 20 days prior to the maximum southerly $\tilde{v}$ flow over the eastern Indian Ocean, the equatorial region around 90°E experiences peak wet condition (O$\tilde{L}$R < 0). These negative O$\tilde{L}$R anomalies then propagate eastward at an average speed of 5 m s^{-1}, reaching the western Pacific between 150°E and the date line at day 0. Similarly, Fig. 5b indicates the importance of southerly $\tilde{v}$ flows along the South African coast upon enhancing eastward propagating equatorial O$\tilde{L}$R perturbations over the Indian Ocean at day 0.

Based on a compositing technique, Murakami (1987) confirmed the occurrence of significant 30–60 day southerlies not only over the Indian Ocean but also along the east coast of South America. This can be reconfirmed by the correlation map for $\tilde{v}$ at lag 0 day (Fig. 4c). Perhaps, this agreement indicates that the correlation maps shown in Fig. 4 are adequate for describing the characteristic features of 30–60 day meridional wind fluctuations over the southern hemisphere. In Fig. 4c, anomalous southerlies along the east coast of South America penetrate equatorward, probably enhancing convection over the northern Brazil–Venezuela region. Thus, this region can be identified as an energy source region for equatorial 30–60 day perturbations. However, this source region becomes active only during a brief period of time around day 0 over a limited area from about 90°W to 50°W. Presumably, this region does not contribute as effectively as the Indian Ocean to the enhancement of planetary-scale 30–60 day perturbations. Yet another feature of interest in Fig. 4c is the presence of anomalous northerlies (southerlies) over the South (North) Pacific. This results in anomalous low-level divergence (below normal convection) over the equatorial central Pacific at day 0 when an active monsoon occurs over central India (reference point). Conversely, the equatorial central Pacific is characterized by anomalous low-level convergence (above normal convection) during break monsoons over central India.

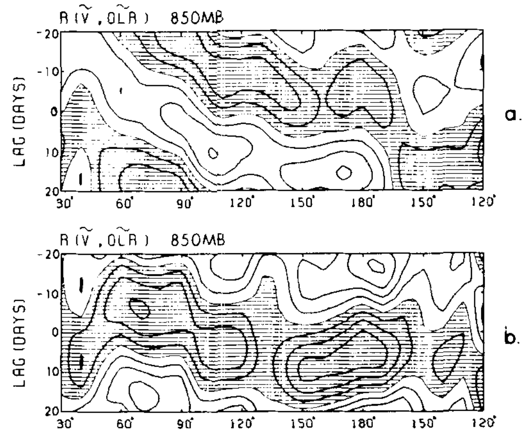

Fig. 5. Lag-longitude sections of lag correlation coefficient between O$\tilde{L}$R, averaged between the equator and 10°N, with reference to the averaged $\tilde{v}$ over (a) the eastern Indian Ocean (100°–110°E, 30°–40°S) and (b) the east African coast (40°–60°E, 10°–20°S). Intervals are 0.2 and negative regions are shaded.

5. Relationship between transient eddies and 30–60 day oscillations

There is no correlation between transient disturbances and low-frequency perturbations due to the orthogonality with different periods (see eq. (2)). However, it is conceivable that the low-frequency modes are related to a group of transient disturbances. This possibility is examined in

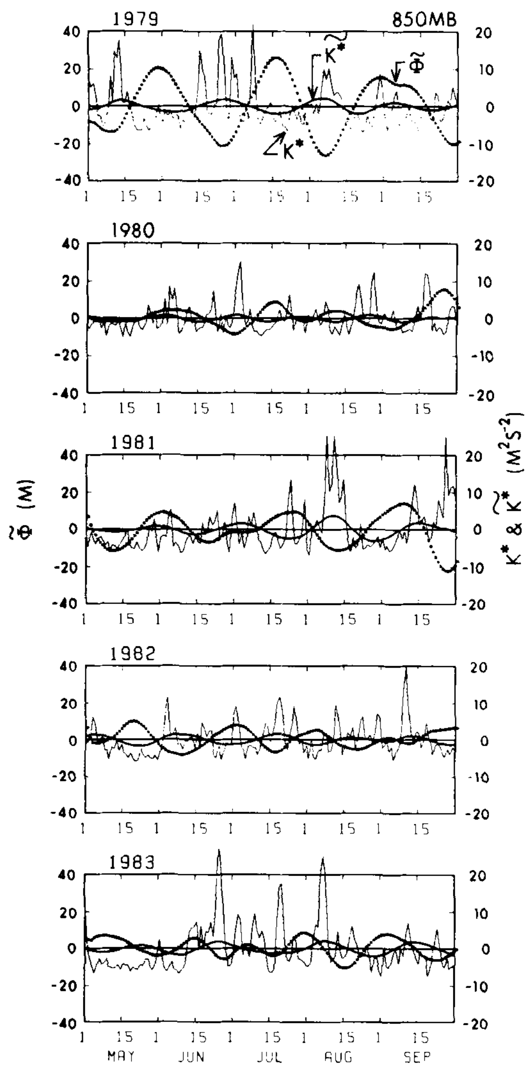

Fig. 6. Time series for k^* (thin full lines; unit: 1 $m^2\ s^{-2}$), $\tilde{k}^*$ (heavy full line; unit: 1 $m^2\ s^{-2}$), and $\tilde{\Phi}$ (heavy dotted line; unit: 1 m) averaged over central India (70°–90°E, 15°–25°N) during the 5 summers (1 May–30 September) of 1979–1983.

this section. First, eddy kinetic energy k^* is calculated as an indicator of the intensity of transient disturbances, i.e., $k^* = (u^{*2} + v^{*2})/2$. The time series of transient k^* (departure from the season mean) at 850 mb (thin full lines) averaged over the monsoon region (70°–90°E, 15°–25°N) during the 5 summers of 1979–1983 are presented in Fig. 6. An inspection reveals a time scale of k^* fluctuations being about 3–10 days. We also see the presence of amplitude modulation. For example, a small k^* amplitude during the period from 15 May to 15 June 1979 is contrasted with a much above normal amplitude from about 15 June to 10 July 1979. Thus, the time scale of k^* variation is definitely much longer than that of transient (u^*, v^*) fluctuations. The results of power spectral analyses for 850 mb k^* over the monsoon region are shown in Fig. 7a. A pronounced spectral peak with a period of about 45 days surpasses the 95% confidence level during the 1979 summer. Similarly, the spectra for k^* are dominated by low-frequency oscillations with periods longer than about 30 days for the 3 summers of 1981–1983. The only exception is the 1980 summer with no significant spectral peak occurring with a period range of 30 to 60 days. However, the western Pacific region is characterized by a well-defined spectral peak with an approximate period of 36 days during the 1980 summer (refer to Fig. 7b).

Having established the presence of low-frequency k^* variations, we then applied a 30–60 day band-pass filter to obtain $\tilde{k}^*$ time-series data. As shown in Fig. 6 for the 1979 summer, an approximate inverse relationship exists between 30–60 day filtered $\tilde{k}^*$ (heavy full line) and $\tilde{\Phi}$ (heavy dotted line). Similarly, $\tilde{k}^*$ is approximately out of phase with $\tilde{\Phi}$ during the four summers of 1980–1983. Undoubtedly, this is an indication of strong interaction of transient synoptic-scale (u^*, v^*) disturbances with 30–60 day planetary-scale $\tilde{\Phi}$ oscillations.

So much for the discussion pertaining to the time scale of k^* perturbations. To facilitate further study on the space scale, we computed the simultaneous correlation between 30–60 day filtered $\tilde{k}^*$ and $\tilde{\Phi}$ at every grid point, which is denoted as $r(\tilde{k}^*, \tilde{\Phi})$. In Fig. 8a, note the predominance of negative correlation less than -0.3 (significant at 95% confidence level) over Southeast Asia and the subtropical western Pacific. Namely, over these monsoon regions, transient perturbations tend to be prominent (large $\tilde{k}^*$) during the active monsoon phase of $\tilde{\Phi} < 0$, while their activity is depressed (small $\tilde{k}^*$) during the break monsoon phase with positive $\tilde{\Phi}$. Although the space scale of transient monsoon disturbances is about 6000 km, a group of time- and space-clustering monsoon disturbances probably facili-

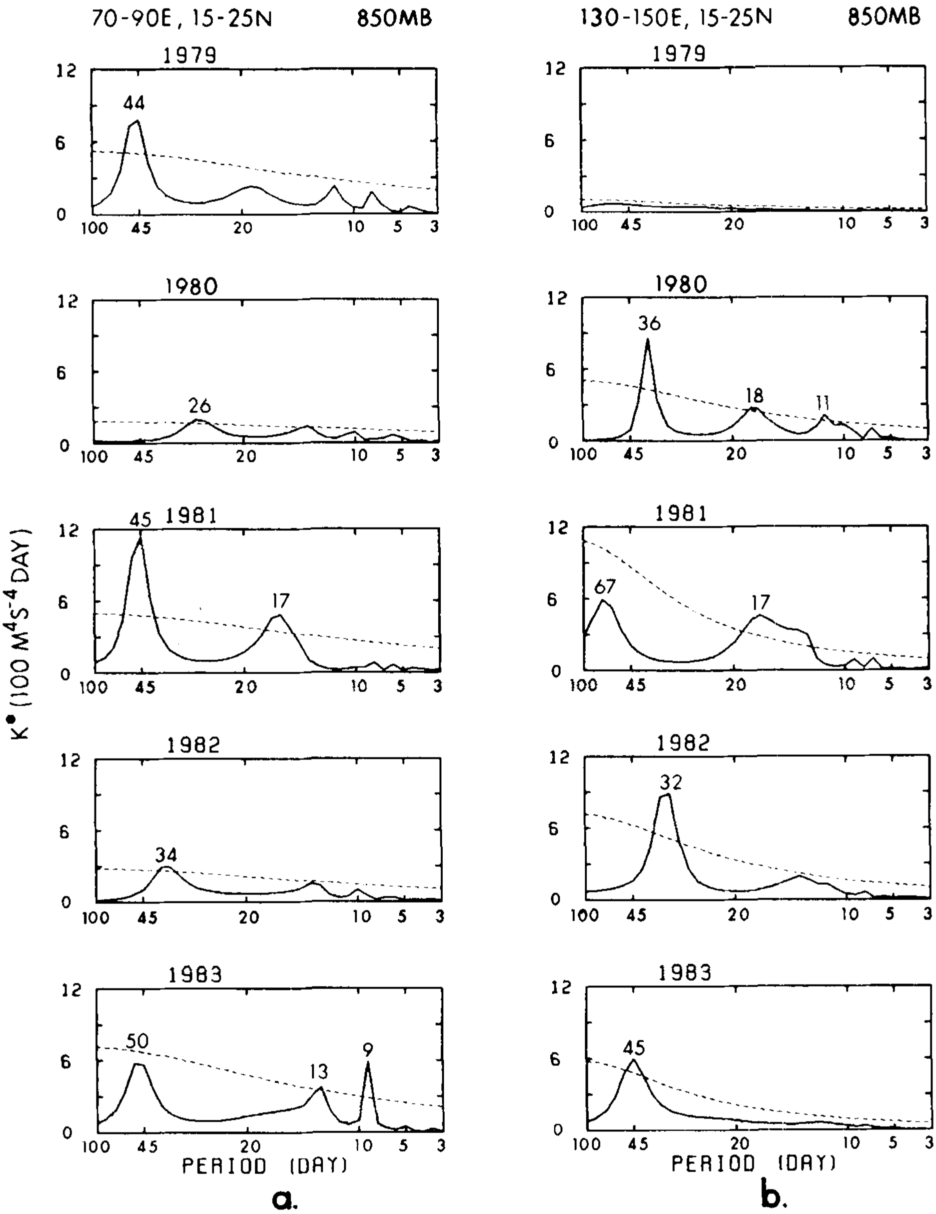

Fig. 7. Power spectra (m^4 s^{-4} day) for daily transient eddy kinetic energy (k^*) at 850 mb. Left: over central India (70°-90°E, 15°-25°N). Right: over the western Pacific (130°-150°F, 15°-25°N).

tates the enhancement of 30–60 day planetary-scale wavenumber 1 perturbations. As emphasized earlier, the interaction with the southern hemisphere mid-latitudes via southerly $\tilde{v}$ flows (anomaly) also contribute to the amplification of low-frequency perturbations over the monsoon region. This amplification, in turn, favors the further intensification of transient monsoon disturbances. These disturbances induce convective activity which, as a group, provides the energy

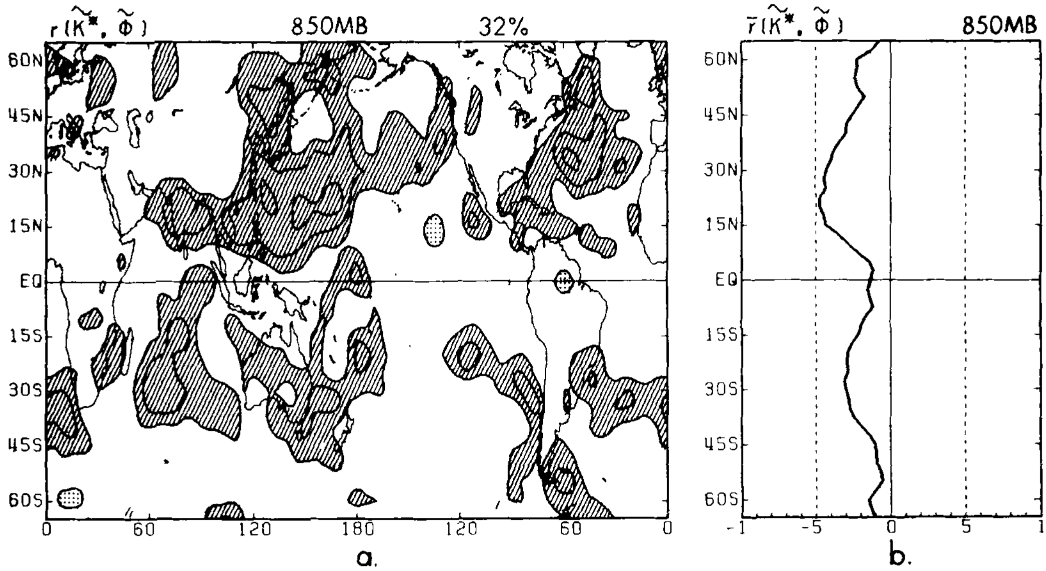

Fig. 8. Left: Simultaneous correlation between $\widetilde{k^*}$ and $\tilde{\Phi}$ at 850 mb. Intervals are 0.2 and regions greater (less) than 0.3 (−0.3) are stippled (hatched). Also shown is the areal percentage that surpasses the local 95% confidence level of ±0.3. Right: Zonally averaged correlation.

for fostering the development of many more synoptic-scale monsoon disturbances. Thus, via these mutual interactions with transient disturbances and convective cells, low-frequency (30–60 day) perturbations become most prominent over the monsoon region.

A similar inverse relationship between $\widetilde{k^*}$ and $\tilde{\Phi}$ also exists over a substantial portion of the southern hemisphere extratropics (Fig. 8a). Over this region, the typical zonal wavenumber for transient baroclinic (u^*, v^*) perturbations is about 5 to 7 (Fig. 2). Since they are internally enhanced within the baroclinic zone, they can be identified as "normal" modes of the southern hemisphere mid-latitude region. No correlation exists between these baroclinic waves and mid-latitude low-frequency modes because of the difference in the time and space scale. However, a group of time- and space-overlapping baroclinic disturbances exhibits a significant correlation with the mid-latitude low-frequency modes (Fig. 8a). This, in turn, indicates that nonlinear coupling with transient baroclinic waves is, at least partially, responsible for the maintenance of southern hemisphere mid-latitude, wintertime low-frequency modes.

In Fig. 8a, the areal percentage that surpasses the local 95% confidence level is about 32%. Fig. 8b shows the zonally averaged correlation, i.e., $\bar{r}(\widetilde{k^*}, \tilde{\Phi})$. As expected, it is less than −0.3 over the northern hemisphere extratropics (10°–40° N) as well as over the southern hemisphere extratropics (15°–40° S). Since the dominant space scale of $\tilde{\Phi}$ is about zonal wavenumber 1 (see Fig. 3c), the characteristic space scale of $\widetilde{k^*}$ should also be approximately zonal wavenumber 1. This can be seen more clearly by plotting $\widetilde{k^*}$ as a function of longitude (not shown). Quite recently, Yamazaki and Murakami (1987) applied the Maximum Entropy Method to daily amplitude value for transient disturbances, which is proportional to k^*. Following the representation of Hayashi (1977) for separating the spectra into eastward and westward moving components for each zonal wavenumber, they found a pronounced spectral peak of eastward propagating wavenumber 1 component with a period range of about 30 to 60 days for the transient disturbance amplitude modulation. Namely, $\widetilde{k^*}$ propagates eastward with the same phase speed as the low-frequency $\tilde{\Phi}$ modes with typical space-scale of wavenumber 1.

In the equatorial zone from about 10°S to 10°N, $\bar{r}(\widetilde{k^*},\tilde{\Phi})$ is small and statistically insignificant, indicating that equatorial low-frequency modes do not interact with transient equatorial disturbances. As mentioned earlier, Hayashi and Sumi (1986) identified the equatorial low-frequency oscillations as "normal" modes, which are internally enhanced and/or self-sustained by convection in the equatorial region. Hence, nonlinear coupling with transient disturbances contributes little to the enhancement of equatorial low-frequency modes. As shown in Fig. 3c, the atmospheric teleconnection between the equatorial and mid-latitude low-frequency modes is characterized by a typical space scale of zonal wavenumber 1.

Since $\tilde{\Phi}$ is of questionable accuracy over the equatorial region, simultaneous correlations were also computed for 30–60 day filtered streamfunction $\tilde{\Psi}$, which was obtained from observed $(\tilde{u},\tilde{v})$ wind fields. It turns out that $r(\widetilde{k^*},\tilde{\Psi})$ [or $\bar{r}(\widetilde{k^*},\tilde{\Psi})$] is essentially identical to $r(\widetilde{k^*},\tilde{\Phi})$ [or $\bar{r}(\widetilde{k^*},\tilde{\Phi})$] and, thus, is not reproduced here. Refer also to Fig. 8 of Murakami et al. (1984) and Fig. 6 of Murakami et al. (1986b) for the association of $\widetilde{k^*}$ with 30–60 day filtered moisture and outgoing longwave radiation fields.

6. Conclusion

Using outgoing longwave radiation (OLR) and 850 mb wind data, the relationship between intraseasonal (30–60 day) meridional wind fluctuations over the southern hemisphere middle latitudes and the low-frequency convective activity over the Asian monsoon region during E phase was investigated. In addition, the interaction between transient disturbances and 30–60 day oscillations was also explored.

Transient disturbances in this paper refer to all the perturbations with periods less than 30 days. In general, the correlation maps for transient disturbances display a regional character. Over the Indian Ocean–Australia region these disturbances show a systematic eastward propagation of 10 m s^{-1} with a wavelength of about 6000 km. This feature reflects the nature of baroclinic disturbances over the southern hemisphere mid-latitudes.

In contrast to these transient disturbances, the correlation patterns for 30–60 day filtered geopotential height field distinctly show a global scale character with a zonal wavenumber one. It has been noted that Baiu activity over southern China and Japan is below normal about 10 days prior to the initiation of active monsoons over central India. This can be closely associated with the northward propagation of 30–60 day perturbations across southeast Asia and the western Pacific.

Low-level southerly $\tilde{v}$ flow (anomaly) is an unique feature to the Indian Ocean region. Along the east African coast, it is first formed near northern Madagascar, and then shows a systematic northward propagation. This southerly flow, after crossing the equator, seems to intensify the monsoonal westerlies near south India, eventually enhancing the convective activity over the entire Asian monsoon region. In comparison, southerly $\tilde{v}$ flows off the west coast of Australia tend to activate convection over the western equatorial Pacific. No significant 30–60 day meridional wind fluctuations occur during NE phase (not shown). Except for the western Indian Ocean, southerly flows (anomaly) do not penetrate equatorward, but are generally confined poleward of about 30°S during NE phase.

There is an indication of a close relation between transient disturbances and 30–60 day oscillations. Transient disturbances over central India have a typical periodicity of about 3–10 days. A noteworthy feature is the amplitude modulation of these transient eddies with a period of about 45 days. Over the monsoon region transient disturbances are prominent during the active monsoon phase. Although no correlation exists between the transient disturbances and the 30–60 day perturbations, a group of time- and space-clustering monsoon disturbances probably facilitates the enhancement of 30–60 day planetary-scale perturbations. Thus, it may be possible that the transient disturbances can be a major energy source for the low-frequency oscillation over the northern hemisphere summer monsoon region. Amplitude modulation is also observed over the mid-latitude Indian Ocean–Australian region.

7. Acknowledgements

The authors are indebted to Mrs. Dixie Zee for her assistance in final editing this manuscript. This research has been supported jointly by the National Science Foundation and the National Oceanic and Atmospheric Administration, Washington, DC, under the Research Grant ATM-8609968.

REFERENCES

Davis, R. E. 1976. Predictability of sea surface temperature and sea level pressure anomalies over the north Pacific Ocean. *J. Phys. Oceanogr. 6*, 249-266.

Hayashi, T. 1977. Space-time power spectral analysis using the maximum entropy method. *J. Meteorol. Soc. Japan 55*, 415-420.

Hayashi, Y. and Sumi, A. 1986. The 30-40 day oscillations in an "aqua planet" model. *J. Meteorol. Soc. Japan 64*, 451-467.

Knutson, T. R., Weickmann, K. M. and Kutzbach, J. E. 1986. Global-scale intraseasonal oscillations of outgoing longwave radiation and 250 mb zonal wind during northern hemisphere summer. *Mon. Wea. Rev. 114*, 605-623.

Krishnamurti, T. N. and Subrahmanyam, D. 1982. The 30-50 day mode at 850 mb during MONEX. *J. Atmos. Sci. 39*, 2083-2095.

Krishnamurti, T. N., Jayakumar, P. K., Sheng, J., Surgi, N. and Kumar, A. 1985. Divergent circulations on the 30-50 day time scale. *J. Atmos. Sci. 42*, 364-375.

Lau, K.-M. and Chan, P. H. 1985. Aspects of the 40-50 day oscillation during the northern hemisphere winter as inferred from outgoing longwave radiation. *Mon. Wea. Rev. 113*, 1889-1909.

Lau, K.-M. and Phillips, T. J. 1986. Coherent fluctuations of extratropical geopotential height and tropical convection in intraseasonal time scales. *J. Atmos. Sci. 43*, 1164-1181.

Lorenc, A. C. 1984. The evolution of planetary scale 200 mb divergence during the FGGE year. *Q. J. R. Meteorol. Soc. 110*, 427-441.

Madden, R. A. and Julian, P. R. 1971. Detection of a 40-50 day oscillation in the zonal wind in the tropical Pacific. *J. Atmos. Sci. 28*, 702-708.

Madden, R. A. and Julian, P. R. 1972. Description of global scale circulation cells in the tropics with a 40-50 day period. *J. Atmos. Sci. 29*, 1109-1123.

Murakami, M. 1979. Large-scale aspects of deep convective activity over the GATE area. *Mon. Wea. Rev. 107*, 994-1013.

Murakami, M. 1984. Analysis of deep convective activity over the western Pacific and southeast Asia. Part II. Seasonal and intraseasonal variations during northern hemisphere summer. *J. Meteorol. Soc. Japan 62*, 88-108.

Murakami, T. 1987. Intraseasonal atmospheric teleconnection pattern during the northern hemisphere summer. *Mon. Wea. Rev. 115*, 2133-2154.

Murakami, T., Nakazawa, T. and He, J. 1984. On the 40-50 day oscillations during the 1979 northern hemisphere summer. Part I: Phase propagation. *J. Meteorol. Soc. Japan 62*, 440-468.

Murakami, T. and Nakazawa, T. 1985. Tropical 45 day oscillation during the 1979 northern hemisphere summer. *J. Atmos. Sci. 42*, 1107-1122.

Murakami, T., Chen, L.-X., Xie, A. and Shrestha, M. L. 1986a. Eastward propagation of 30-60 day perturbations as revealed from outgoing longwave radiation data. *J. Atmos. Sci. 43*, 961-971.

Murakami, T., Chen, L.-X. and Xie, A. 1986b. Relationship among seasonal cycles, low-frequency oscillations, and transient disturbances as revealed from outgoing longwave radiation data. *Mon. Wea. Rev. 114*, 1456-1465.

Sikka, D. R. and Gadgil, S. 1980. On the maximum cloud zone and ITCZ over Indian longitudes during the southwest monsoon. *Mon. Wea. Rev. 108*, 1840-1853.

Yamazaki, N. and Murakami, M. 1987. An intraseasonal amplitude modulation of the short-term tropical disturbances over the western Pacific. *J. Meteorol. Soc. Japan*, October issue.

Yasunari, T. 1980. A quasi-stationary appearance of 30-40 day period in the cloudiness fluctuations during the summer monsoon over India. *J. Meteorol. Soc. Japan 58*, 225-229.

Yasunari, T. 1981. Structure of an Indian summer monsoon system with around 40-day period. *J. Meteorol. Soc. Japan 59*, 336-354.

Yasunari, T. 1986. Low-frequency interactions between the summer monsoon and the northern hemisphere westerlies. *J. Meteorol. Soc. Japan 64*, 693-708.